

Theory for rates, equilibrium constants, and Brønsted slopes in F_1 -ATPase single molecule imaging experiments

Sándor Volkán-Kacsó and Rudolph A. Marcus¹

Noyes Laboratory of Chemical Physics, California Institute of Technology, Pasadena, CA 91125

Contributed by Rudolph A. Marcus, September 17, 2015 (sent for review August 25, 2015; reviewed by Attila Szabo and Arieh Warshel)

A theoretical model of elastically coupled reactions is proposed for single molecule imaging and rotor manipulation experiments on F_1 -ATPase. Stalling experiments are considered in which rates of individual ligand binding, ligand release, and chemical reaction steps have an exponential dependence on rotor angle. These data are treated in terms of the effect of thermodynamic driving forces on reaction rates, and lead to equations relating rate constants and free energies to the stalling angle. These relations, in turn, are modeled using a formalism originally developed to treat electron and other transfer reactions. During stalling the free energy profile of the enzymatic steps is altered by a work term due to elastic structural twisting. Using biochemical and single molecule data, the dependence of the rate constant and equilibrium constant on the stall angle, as well as the Brønsted slope are predicted and compared with experiment. Reasonable agreement is found with stalling experiments for ATP and GTP binding. The model can be applied to other torque-generating steps of reversible ligand binding, such as ADP and P_i release, when sufficient data become available.

biomolecular motors | free energy relations | ATPase | single molecule imaging | Brønsted slope

Single molecule imaging directly demonstrated a stepping rotation in F_1 -ATPase (1) that was resolved into $\sim 40^\circ$ and $\sim 80^\circ$ substeps (initially reported as $\sim 30^\circ$ and $\sim 90^\circ$; cf. refs. 2 and 3), and much information has been extracted by elaborate techniques at the single molecule level (3–6). Complementing experimental tools such as X-ray spectroscopy (7) and ensemble biochemical methods (8), single molecule experiments reveal key details of the coupling between enzymatic processes and rotation (9–12). A detailed picture of highly coordinated substeps has emerged in which the binding of solution ATP to an empty subunit and release of hydrolyzed ADP from the clockwise neighbor (viewed from the rotor side) occur in concert during the $\sim 80^\circ$ rotation step (13). As depicted in Fig. 1 and Table 1, the subsequent $\sim 40^\circ$ rotation is coordinated with the hydrolysis of ATP in the third subunit and the release of P_i from the subunit that just released ADP (13).

Recent stalling (6, 13, 14) and controlled rotation (15) experiments provide additional insight into the dynamics of the coupling between the rotation of the central shaft and the reaction steps in the stator ring subunits. These experiments yielded the rate constants of various steps, binding and release of ligands, and hydrolysis/synthesis reaction, as a function of the stalled rotor angle θ . The rates show an exponential dependence on θ over a wide range, such as a range of 80° for ATP binding and 40° for hydrolysis. Free energy profiles for the initial and final dwell angles at a specific 40° or 80° step are given in Fig. 2. For intermediate stalling angles, the profile is intermediate between these two limits.

In stalling experiments (14) the freely rotating shaft of the ATPase is stalled by magnetic tweezers upon reaching a dwell angle. Rotation experiments have resolved two dwells: the binding dwell (before the 80° step) and the hydrolysis dwell (before the 40°

step). The rotor was stalled at various θ s around each of these dwell angles for a predetermined time, then was released. The system immediately returned either to the original dwell angle or went forward to the next dwell angle, depending on the state of the underlying process at the moment of release. The observed relative number of forward and back events as a function of stall time was given a simple two-state kinetic interpretation (14), which in turn permitted the determination of forward and backward rate constants of ATP binding, ATP hydrolysis, and P_i release. In the present article we formulate a theory for predicting the dependence of the rate constant and equilibrium constant on the stalling angle for the binding and release steps.

In a different set of experiments (15), a slow, controlled rotation of the shaft was performed by magnetic tweezers. The change in the ligand occupancy was monitored as a function of the rotor angle using fluorescent ATP and ADP analogs. Events whereby the occupancy changed between 0 and 1 were identified following an intuitive “grouping” criterion and subsequently analyzed. The number of ($0 \rightarrow 1$) and ($1 \rightarrow 0$) events over the time spent in a 0 and 1 occupancy state yielded forward and reverse rate constants, respectively. In both types of experiments the equilibrium constant (K) was calculated as the ratio of forward rate constant (k_f) and reverse rate constant. In what follows we focus on the stalling experiments that use a straightforward method for rate versus θ data estimation that do not require a grouping criterion.

Theory for F_1 -ATPase Experiments

A Brønsted Interpretation of Single Molecule Data. In the interpretation proposed here for treating these single molecule stalling experiments the rate dependence can be translated, assuming transition state (TS) theory and using thermodynamics, into free energy relations (cf. Fig. 2). For the forward reaction rate constant

Significance

The biological function in the F_1 -ATPase enzyme can be elucidated by understanding the dynamical interplay of reactions and mechanical rotation in the protein. Recent single molecule imaging and rotor manipulation experiments revealed that the rate constants of enzymatic steps, such as ATP binding or phosphate release, show an exponential dependence on the stalled rotor angle. Following concepts that originated in theories of electron and group transfer reactions, a structure-based analytic model is described to treat the dynamical behavior observed in these experiments. Using biochemical and the single molecule observations, thermodynamic driving potentials are constructed that take into account the elasticity of the rotor shaft. The model predicts observable quantities without using adjustable parameters and is tested using existing data.

Author contributions: S.V.-K. and R.A.M. designed research; S.V.-K. and R.A.M. performed research; S.V.-K. analyzed data; and S.V.-K. and R.A.M. wrote the paper.

Reviewers: A.S., National Institutes of Health; and A.W., University of Southern California.

The authors declare no conflict of interest.

See Commentary on page 14121.

¹To whom correspondence should be addressed. Email: ram@caltech.edu.

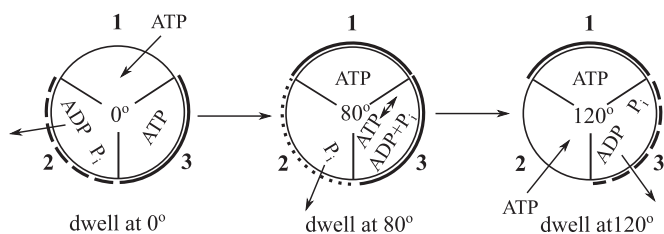


Fig. 1. Scheme of coupled processes in F_1 -ATPase during free rotation. The dwell angle increases in the counter clockwise direction. The species occupying the pockets of ring β subunits 1, 2, and 3 are represented in the binding and catalytic dwells. The thick arcs represent a closed subunit structure preventing admission or release of cited species. Dashed lines indicate that the structure opens up during the step to allow release of the specified species. The conformational change corresponding to ATP binding/release (long dashes) is a hinge-bending motion (47), and that corresponding to P_i release/rebinding (short dashes) is a different, less pronounced rearrangement (48).

$k_f(\theta)$ and the equilibrium constant $K(\theta)$ of a given reaction step we write

$$k_f(\theta) = (kT/h)\exp[-\Delta G^\ddagger(\theta)/kT], \quad [1]$$

$$K(\theta) = \exp[-\Delta G_s^0(\theta)/kT], \quad [2]$$

where $\Delta G^\ddagger(\theta)$ and $\Delta G_s^0(\theta)$ are the Gibbs free energy of activation and the standard free energy of reaction, respectively, for that step. Thus, the exponential rate dependences with respect to each angle θ in experiments (14, 15) correspond to free energy relations and provide the Brønsted slope α (16–18), defined by

$$\alpha = \frac{\partial \ln k_f(\theta)}{\partial \ln K(\theta)} = \frac{\partial \Delta G^\ddagger}{\partial \Delta G_s^0} \quad [3]$$

at any given T (Table 2). Depending on the position of the TS along a reaction coordinate, α can vary from 0, if the TS is reactantlike, to 1, if the TS is productlike. Otherwise, α takes on intermediate values within these limits, in particular $\sim 1/2$ if ΔG^0 is small relative to a reorganization energy defined later. Because the Brønsted slope α is approximately constant within a limited range of free energies, the equivalent of Eq. 3 in the literature is often termed as a linear free energy relation. In effect, α also serves as a measure for the position of the TS along a reaction coordinate. In the present case of the F_1 -ATPase we treat the free energies involved, after the first contact of ATP with the ATPase, with the transition from one set of hydrogen bonds linking the ATP to the ATPase, to another set.

Reaction Theory with Structural Elasticity. A goal here is to calculate rate and equilibrium constants and their dependence on the rotor angle for the binding of ligand molecules in the stalled F_1 -ATPase system. To this end we use a formalism originally introduced for electron (19) and other transfers, including hydrogen [proton (20), hydride, and H-atom] and even methyl cation (21) transfers. In this formalism, when the reactants approach each other to some separation distance R , there is a “work term” $w^r(R)$, including any electrostatic interaction and/or structural reorientation. [In the electron transfer theory there is a weighted integral over a separation distance coordinate R involving an electronic transition probability $p(R)$, the pair distribution function of the reactants $g(R)$, and the dependence of $\Delta G^\ddagger(R)$ on R (22–24).] This work is then, in the theory, followed by the reaction, which includes any chemical or other structural changes, and in turn followed by a separation of the products from R to ∞ , involving a work term, $-w^p(R)$ (16). The standard free energy of reaction at that R denoted by $\Delta G^0(R)$ is then given by $\Delta G^0(R) = \Delta G^0 + w^p(R) - w^r(R)$, where ΔG^0 is the standard free energy of reaction at $R = \infty$. In this formalism, the free energy of activation ΔG^\ddagger is given by (16)

$\Delta G^\ddagger(R) = w^r(R) + [\lambda + \Delta G^0(R)]^2/4\lambda$, where λ is the reorganization energy for the reaction. [A closely related equation, based instead on a bond energy–bond order model, is given in ref. 16. A resonance correction to the equation for $\Delta G^\ddagger(R)$ for strong overlap reactions is given in ref. 25.]

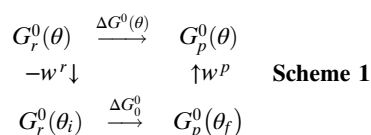
We apply these concepts to a reaction step in F_1 -ATPase noting that the stalling angle θ plays the role of R in the equations for $\Delta G^0(R)$ and $\Delta G^\ddagger(R)$. In particular, we consider the binding of ATP or an ATP analog to the binding pocket, because for this process there are currently the most extensive stalling experimental data. (Hereafter, as customary, ATP, ADP and any analog will denote the molecule coordinated with a Mg^{2+} ; refs. 26 and 27). Nevertheless, the general features of the model are intended to apply also to other rotation-coupled steps involving the reversible binding and release of a ligand molecule, such as ADP and P_i , and to other ring-shaped NTPases, and can be tested once sufficient kinetic data become available. The model, as presently formulated, does not apply to the ATP hydrolysis (cleavage) step, because it may be a multistep process (28–30), as discussed in more detail in a later section.

Initially, before any reaction occurs, the rotor angle is changed from its initial equilibrium angle (dwell angle) θ_i to some value of the stalled angle θ . This change has been induced by turning on the magnetic field of the “tweezers”: the magnetic bead attached to the rotor tip aligning itself with the direction of this external magnetic field. Under this condition the system is still in the reactant state, because the ATP in solution has not yet bound and the subunit is in the open state. Because the stator ring is anchored to the surface of the reaction vessel acting as a stator, the rotor shaft, and to some extent the whole structure, undergoes a twisting deformation when θ is changed from θ_i . The work done by the magnetic field to achieve this deformation is denoted by $w^r(\theta)$.

The equilibrium value of θ after the reaction occurs and the magnetic field is turned off is denoted by θ_f , another dwell angle. The work done by the F_1 -ATPase during the untwisting of the rotor upon turning off the magnetic field is then $w^p(\theta)$. Assuming a harmonic twisting of the F_1 -ATPase rotor–stator complex (6, 31, 32) with a torsional elastic constant κ , we have for any stalling angle θ ,

$$w^r = \frac{\kappa}{2}(\theta - \theta_i)^2, \quad w^p = \frac{\kappa}{2}(\theta - \theta_f)^2. \quad [4]$$

Using work terms one can build a thermodynamic cycle to calculate the standard free energy of reaction while the system is stalled at an angle θ .



In Scheme 1 $G_r^0(\theta)$ and $G_p^0(\theta)$ denote the free energies of the system in its reactant and product states at the stalled angle θ ,

Table 1. Representation of the steps in the sequential relay mechanism of rotation in F_1 -ATPase

$\theta_i \dots \theta_f$ ($^\circ$)	β_1 subunit	β_2 subunit	β_3 subunit
0 ... 80	ATP binding	ADP release*	ATP in pocket
80 ... 120	ATP in pocket	P_i release	ATP hydrolysis [†]
120 ... 200 [‡]	ATP in pocket	ATP binding	ADP release*

In the stator ring the $\beta_1, \beta_2, \beta_3$ order is counter clockwise as viewed from the rotor side. Key subunit for the step are in boldface. The “ATP, ADP and P_i in pocket” fields correspond to no ligand change during this step.

*ADP release is irreversible in these experiments and does not affect the outcome of stalling experiments.

[†]We neglect the effect of the coupling of the hydrolysis cleavage reaction to rotor.

[‡]This transition is identical to that of $\theta_i = 0^\circ$ (first row) if the ring is rotated by 120° counter clockwise.

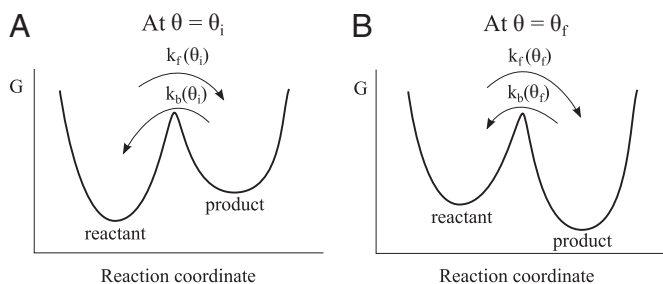


Fig. 2. Dependence of forward and reverse rates and free energy profiles on the stalling angle θ for a given step. The two cases represented correspond to a stall angle set at (A) the initial (reactant) angle θ_i and (B) the final (product) angle θ_f . For other stall angles $\theta_i < \theta < \theta_f$ the profiles are intermediate between a and b. The value of θ_i and θ_f for the different steps are given in Table 1. For the ATP binding step, in the reactant state an ATP molecule is weakly bound to the entrance of the open subunit, and in the product state the molecule is bound to the internal pocket site of the closed subunit. This subunit is structurally coupled to the rotor shaft and produces rotation if the latter is unobstructed, but if the rotor is stalled, a binding transition results in an elastic distortion of the system.

and $G_r^0(\theta_i)$ and $G_p^0(\theta_f)$ are the corresponding standard free energies of the elastically relaxed or freely rotating system at θ_i and θ_f , respectively. The arrows denote the direction of the free energy changes and work terms from one state to another. Scheme 1 is analogous to the equation for $\Delta G^0(R)$ above, if θ and R are interchanged. From Eq. 4 and Scheme 1 it follows that the contribution to $\Delta G^0(\theta)$ for the F_1 -ATPase system due to elastic twisting of the rotor, and the rotor tip is stalled at an angle θ , is $w^p(\theta) - w^r(\theta)$, and thereby

$$\Delta G^0(\theta) = \Delta G_0^0 - \kappa(\theta_f - \theta_i) \left[\theta - (\theta_f + \theta_i)/2 \right], \quad [5]$$

where ΔG_0^0 , as defined in Scheme 1, is the standard free energy of reaction for the freely rotating system, $\Delta G_0^0 = G_p^0(\theta_f) - G_r^0(\theta_i)$. We note in passing that θ is a parameter and not a reaction coordinate, as discussed below.

For the binding of ATP to the ATPase we note that there is a term involved in the binding (27) to the outside or “entrance” of the empty subunit, which we denote by W^r (we note also the distinction between w^r and W^r). In that case the effective free energy barrier that the ATP molecule needs to overcome will include this initial binding contribution,

$$\Delta G^\ddagger(\theta) = W^r + [\lambda + \Delta G^0(\theta)]^2 / 4\lambda, \quad [6]$$

where $\Delta G^0(\theta)$ is given by Eq. 5. Although we use for simplicity the two-parabola basis of the quadratic relation in Eq. 6, the equation represents approximately a more general relation and has been tested by detailed quantum mechanical electronic structure calculations (e.g., 33–37).

To obtain an expression for the forward reaction rate constant k_f for ATP binding we note that there is a rate constant for the solution ATP reaching the ATPase, namely, a collision frequency Z . The rate constant for binding to the inside of the pocket is then this Z multiplied by $\exp(-W^r/kT)$ and by $\exp[-(\lambda + \Delta G^0(\theta))^2 / 4\lambda kT]$, the “reaction term” for transitioning into the pocket, according to Eq. 6. Thereby, k_f is given by:

$$k_f(\theta) = Z \exp[-\Delta G^\ddagger(\theta)/kT]. \quad [7]$$

(The derivation of a Z -based Eqs. 7 and 8 from a kT/h based Eq. 1 can be seen in ref. 22, their equation 31, and involves converting a free energy contribution associated with the approach of the two reactants from solutions.) Any orientational restrictions on the ATP in binding to the outside of the ATPase are included in the W^r . Here, $\Delta G^\ddagger(\theta)$ is given by the quadratic expression in

Eq. 6. For a sufficiently broad range of G^0 's of the reaction series, such curved free energy plots and Brønsted plots predicted in Eq. 6 (or its R -dependent analog) have been reported in experimental (38) and computer simulated (39, 40) electron transfer reactions. In analogy, we denote by k_{f0} the rate constant of the reaction for the freely rotating system,

$$k_{f0} = Z \exp[-\Delta G_0^\ddagger/kT], \quad [8]$$

ΔG_0^\ddagger being the free energy of activation,

$$\Delta G_0^\ddagger = W^r + [\lambda + \Delta G_0^0]^2 / 4\lambda. \quad [9]$$

From Eqs. 5, 6, and 7 one finds that k_{f0} and ΔG_0^\ddagger are equal to $k_f(\theta)$ and $\Delta G^\ddagger(\theta)$ evaluated at $\theta = (\theta_i + \theta_f)/2$, a result we use in *Results*.

To obtain an expression for the equilibrium constant $K(\theta)$ we note that $\Delta G_s^0(\theta)$ is the Gibbs standard free energy of reaction assuming a reactant state where ATP is in solution, standard conditions (1 mol/l). Then $G^0(\theta)$, the standard free energy of the reactant state of binding transition, where the ATP already bound to the entrance site of the open subunit is $\Delta G_s^0(\theta)$ minus any work and entropic terms to bring ATP to the contact point,

$$\Delta G^0(\theta) = \Delta G_s^0(\theta) - W^r - kT \ln kT/hZ. \quad [10]$$

By analogy, for free rotation ΔG_{f0}^0 denotes the Gibbs standard free energy of reaction for a reactant state where ATP is in solution (1 mol/l), and we have

$$\Delta G_{f0}^0 = \Delta G_{s0}^0 - W^r - kT \ln kT/hZ. \quad [11]$$

Several predictions result from these equations:

1. $\ln K(\theta)$ is predicted to be a linear function of θ with a slope of $\kappa(\theta_f - \theta_i)$, according to Eqs. 2, 5, and 10. The numerical value of the slope can be predicted from the measured values of κ and $(\theta_f - \theta_i)$, and compared with values obtained from the stalling experimental measurements. Alternatively, the experimental slope and $(\theta_f - \theta_i)$ values can be used to predict the elastic constant κ .
2. The $\ln k_f(\theta)$ given by Eqs. 6 and 7 is predicted to be an approximately linear function of θ in the range of $-(\theta_f - \theta_i)/2 < \theta - \theta_i < (\theta_f - \theta_i)/2$ probed in stalling experiments. The slope of the linear function depends on G_0^0 , λ and W^r , which can be estimated independently, as below, from experiment. Concomitantly, within this angular range $\Delta G^\ddagger(\theta)$ obeys an approximate linear free energy relation.
3. The Brønsted slope α defined in Eq. 3 is given by

$$\alpha = \frac{d \ln k_f(\theta)/d\theta}{d \ln K(\theta)/d\theta} = \frac{1}{2} + \frac{\Delta G_0^0}{2\lambda} - \frac{\kappa(\theta_f - \theta_i)}{2\lambda} \left[\theta - \frac{\theta_f + \theta_i}{2} \right]. \quad [12]$$

Typically, when $\Delta G_0^0/\lambda$ is small, α will be close to 0.5. We note that the last term is a small θ -dependent correction to the slope, given the range of stall angles probed in the experiment (14).

4. The present framework is intended to apply to rotor-coupled enzymatic steps involving binding and release of ligand molecules, including ATP binding, ADP binding, and P_i release, with properties specific to each step. In particular for the P_i release step, there is no W^r term but a product work term W^p applies:

$$\Delta G^\ddagger(\theta) = [\lambda + \Delta G^0(\theta)]^2 / 4\lambda - W^p. \quad [13]$$

A coupling between rotor and a ring subunit undergoing the enzymatic step is valid over the range from the R to the P regions, perhaps while hydrogen bonds and other contacts between rotor and β domain are maintained. In the next step, a different rotor- β subunit

coupling applies, as new contacts form and another subunit “drives,” by virtue of the reaction process in it, with the rotor coupled to a new subunit. In unconstrained rotation experiments the sequence of steps results in an effective sequential relay mechanism reminiscent of a previous proposal (41). As depicted in Table 1 θ_i is reset for each step and progressively assumes values of 0° , $\sim 80^\circ$, $\sim 120^\circ$, ... We note that a mechanism that couples the $\alpha_3\beta_3$ ring to the rotor shaft, including the effective spring constant, has been attributed to an electrostatic energy landscape from simulations (42, 43).

Treatment of the Coupled Processes in the 80° Step. In the first row of Table 1 we have two coupled processes, the binding of ATP in one pocket and the release of ADP in a second pocket. These processes may be sequential or synchronous. For the sequential case the ADP release must be very rapid, because it has no effect on ATP binding (14). We give here a formal treatment of coupled events in case they are synchronous, and denote the respective occupancies of the two pockets at time t by $n_1(t)$ and $n_2(t)$. Although n_1 goes from 0 to 1, n_2 goes from 1 to 0, and so $n_1(t) + n_2(t) = 1$ in the synchronous system. For the rates dn_1/dt and dn_2/dt of the kinetic steps the simplest coupling phenomenology is given by

$$\frac{dn_1}{dt} = k_1(1 - n_1)[1 + f(\theta)] \quad [14]$$

$$-\frac{dn_2}{dt} = k_2 n_2[1 - f(\theta)], \quad [15]$$

where k_1 , a pseudo first-order rate constant, denotes the bimolecular rate constant for ATP binding to the ATPase multiplied by the ATP concentration in solution. In these equations the phenomenological dynamic coupling parameter of the two pockets, denoted by $f(\theta)$, accelerates the intrinsically slower step and retards the intrinsically faster step. The k_i s in Eqs. 14 and 15 are $k_i(\theta)$ s.

The net rate J is given by dn_1/dt or by its equivalent $-dn_2/dt$. From the addition of the above two equations, after first dividing each by its k_i , we obtain

$$J \left(\frac{1}{k_1} + \frac{1}{k_2} \right) = 2n_2. \quad [16]$$

The effective rate constant of the coupled pair of processes in this row of Table 1, k , defined by setting $J = k(\theta)n_2$, is given by

$$\frac{1}{k(\theta)} = \frac{1}{2} \left(\frac{1}{k_1(\theta)} + \frac{1}{k_2(\theta)} \right). \quad [17]$$

We see that $k = k_1$ when $k_1 = k_2$, a result understood by recognizing that the pair of coupled reaction equations then becomes equivalent to a single first-order reaction. A second consequence of this equation is that when one of the rate constants (k_1, k_2) is intrinsically much faster than the other, k is essentially equal to the smaller of the two k_i s and so the faster k_i then plays no role. Our inspiration for the coupling formalism in Eqs. 14 and 15 is the treatment of the effective interaction of diffusing ions in solutions, using a diffusion potential analogous to $f(\theta)$ (44).

In the following analysis we note that the pseudo first-order rate constant of the ATP binding step, k_1 , is intrinsically much slower than first-order rate constant k_2 for the ADP release step (3). Accordingly, in our analysis of the two steps in the first row of Table 1, the $k(\theta)$ is that of the ATP binding step, and we focus on it.

Results

Comparison of Stalling Experiments with Theoretical Predictions. According to Eqs. 6 and 12 the theoretically predicted Brønsted slope α is a function of the energetics of the freely rotating system, in particular W^r s, ΔG_0^0 s, and λ s. These energies were estimated from experimental forward and reverse rate constants for both ATP and GTP, and the binding affinities for the empty open-conformation system.

The W^r appearing in Eqs. 6 and 7 is approximately -9.1 kcal/mol for ATP binding, calculated from the binding affinity of -6.3 kcal/mol to the empty open-conformation subunit adjusted for entropic contributions of -2.8 kcal/mol. [The affinity of the ATP to form an outer-complexed state to the ATPase can be regarded as the standard free energy change, starting from unit concentration of ATP in solution, to form an outer bound complex with the ATPase. This free energy in turn can be regarded as the sum of a free energy change to make contact between the ATP and the ATPase plus W^r , the binding free energy of that ATP to the ATPase in this outer bound complex. The former can be shown to equal $-kT \ln kT/hZ$ (cf. ref. 16, their footnote 21), where a ratio of quantities kT/hZ was given, and the desired free energy is $-kT \ln kT/hZ$.] The former corresponding to a dissociation constant of $25 \mu\text{M}$, which was measured by a fluorescent ensemble technique (27). We estimated $\Delta G_0^+ = 5.0$ kcal/mol using Eq. 8 for the freely rotating system, assuming $Z = 10^{11} \text{ M}^{-1} \text{ s}^{-1}$ and using the known value of $k_{f0} = 2 \times 10^7 \text{ M}^{-1} \text{ s}^{-1}$ (3). The collision frequency in solution is approximately equal to the gas phase value multiplied by the hard sphere pair distribution function at contact, a value of about 2–3 (45), incorporated into W^r . Consequently, for the freely rotating system, the overall free energy of activation for the ATP binding transition is estimated to be $\Delta G_0^+ - W^r = 11.3$ kcal/mol.

The ΔG_0^0 for ATP binding is estimated from the free rotation equilibrium constant $K_0 = k_{f0}/k_{b0} \cong 10^9 \text{ M}^{-1}$, noting that $-kT \ln K_0 = \Delta G_0^0$. Because there is no k_{b0} available for the ATP release rate (reverse process), k_{b0} is identified by $k_b(\theta)$ at $\theta = (\theta_i + \theta_f)/2$ from stalling experiments (14) by applying Eqs. 1, 13, and 5 for the release process. If $\Delta G_{s0}^0 = -kT \ln K_0 = -12.3$ kcal/mol, $W^r \cong -9.1$ kcal/mol, and $kT \ln kT/hZ = 2.8$ kcal/mol for a standard state of 1 mol/l, then according to Eq. 11 $\Delta G_0^0 = -6.0$ kcal/mol (cf. Table 3).

An estimate of λ follows from Eq. 9 written for free rotation. Given that for ATP binding $\alpha \approx 0.5$ and thus $\Delta G_0^0 \ll \lambda$ the expansion of the quadratic term yield the approximate solution for λ ,

$$\lambda/4 \cong \Delta G_0^+ - W^r - \Delta G_0^0/2, \quad [18]$$

where the quantities on the right-hand side were obtained above. The procedure for GTP binding energetics is similar, but we note that because currently there is no available free rotation rate k_{f0} data, we used the forward stalling experiments at $\theta = (\theta_f + \theta_i)/2$ to calculate k_{f0} using Eqs. 5, 6, and 8, and assumed that W^r is equal to that for ATP binding.

The Brønsted slopes of various enzymatic steps extracted from stalling and controlled rotation experiments are given in Table 2. To extract Brønsted slopes, the experimentally measured reaction rate and equilibrium constants at a limited range of θ s, given in prediction 2 above gave the values of $\ln k(\theta)$ and $\ln K(\theta)$ functions, that in turn gave an approximately linear plot of $\ln k(\theta)$ vs. $\ln K(\theta)$, yielding the Brønsted slope according to Eq. 3. Thereby, the stalling experiments (14) provided estimates for free energy relations and slopes for ATP and GTP binding (Table 2, entries 1–2), which permitted a quantitative comparison with the predictions of the present theory.

Theory and experiment (14) are compared in Tables 3 and 4 below for the slope of the $\ln k_f(\theta)$ functions, the elastic spring constant κ , and the Brønsted slopes α . The experimental values of α for ATP and GTP binding are equal, within experimental error.

According to Eqs. 7–12, several factors affect the equilibrium constant and forward rate constant slopes, $d \ln K/d\theta$ and $d \ln k_f/d\theta$: the torsional stiffness, the total angular displacement, the reorganization energy, the standard free energy of reaction, and the initial binding energy. In Table 4, we use the energetics from Table 3, the values of $(\theta_f - \theta_i)$ and $d \ln K/d\theta$ to predict $d \ln k_f/d\theta$ and κ . Based on Junge and coworkers' measurements (32) $\kappa = 20 \text{ pN} \cdot \text{nm}$, chiefly due to the rotor compliance.

Extension of the Treatment to P_i Release. In the free rotation of F_1 -ATPase the 40° rotation is coupled with the ATP hydrolysis in one subunit and P_i release from the clockwise neighbor subunit (6), as

summarized in Table 1. The timescales associated with the two processes have been resolved by rotation experiments (46), meaning that they occur consecutively rather than synchronously, but kinetics alone cannot distinguish whether the steps occur in a specific sequential order or simultaneously (3). Meanwhile, for the present purpose of treating P_i release, we neglect the effect of the coupling of hydrolysis with rotation during the 40° step given its small standard free energy of reaction, $\Delta G^0 \cong 0.6$ kcal/mol (27).

Although ideas similar to those for the ATP binding can be adapted to the substep of P_i release, there are presently only two θ -dependent rate data points from previous experiments (3, 6), which prevents an adequate estimation of the analogous $k(\theta)$, $K(\theta)$, and α . We describe, nevertheless, a procedure for treating such data when they become available in systematic angle-dependent experiments.

For P_i release the free rotation ΔG_0^0 and ΔG_0^\ddagger can be estimated using an Eq. 1 analog for release, $\Delta G_0^\ddagger = -kT \ln(hk_{f0}/kT)$, and the forward rate constant $k_{f0} \cong 10^5$ s $^{-1}$; and collision theory for rebinding, i.e., an Eq. 7 analog $\Delta G_0^\ddagger - \Delta G_0^0 = -kT \ln k_{b0}/Z$, with $Z = 10^{11}$ M $^{-1}$ s $^{-1}$ and $k_{b0} \cong 10^5$ M $^{-1}$ s $^{-1}$, a rate constant from stalling experiments (6, 14). Thereby, one obtains $\Delta G_0^0 = 2.8$ kcal/mol and $\Delta G_0^\ddagger = 10.9$ kcal/mol. Here, k_{f0} and k_{b0} were approximated from angle-dependent data at $\theta = (\theta_i + \theta_f)/2$. We neglected any binding effect of the P_i to the exit site just before its release into solution, $W^p \cong 0$. Using the same $\kappa = 20$ pN \cdot nm, $\lambda = 38$ kcal/mol can be calculated using Eq. 13.

P_i release is a major torque-generating step (3, 26, 48), hence we suggest that it is coupled to the rotor in the full range of θ , i.e., $\theta_f - \theta_i \cong 40^\circ$. As noted above hydrolysis has a small standard free energy of reaction, according to both ensemble (32) and single molecule experiments (3). Assuming that in F_1 -ATPase chemomechanical energy transduction can be very efficient (49), the energetics also support the idea of a small hydrolysis-coupled rotation. For P_i release then, considering the given $\theta_f - \theta_i$ value, the theory permits us to predict the θ -dependence of $d \ln K/d\theta = 0.48$ and $d \ln k/d\theta = 0.26$ per 10° of stalling angle, and Brønsted slope of $\alpha = 0.26/0.48 = 0.54$, using Eqs. 3, 5, and 6, as described above. These results then can be compared with experimental counterparts when more data become available.

Concluding Discussion and Outlook

An elastochemical theory of the F_1 -ATPase rotary biomolecular motor described here provides an interpretation and explanation for stalling experiments. The rate dependences on the rotor shaft angle in various substeps are interpreted in terms of free energy relations, and compared with theory. A transition-state treatment based on a theory of electron, atom, proton, and group transfers is given to interpret and predict these relations for ATP and GTP

Table 2. Brønsted slopes of various reaction steps extracted from single molecule experiments in F_1 -ATPase

Number	Reaction step	Deduced slope*	Source of experimental rates
1	ATP binding	$0.48 \pm 0.05^\dagger$	Stalling (14)
2	GTP binding	$0.56 \pm 0.08^\ddagger$	Stalling (14)
3	ATP hydrolysis ‡	(1)	Stalling (14)
4	ATP γ S hydrolysis ‡	(1)	Stalling (14)
5	P_i release	$\sim 0.7^{\S}$	Stalling, free rotation (3, 6)
6	Cy3-ATP binding ¶	$0.4 - 0.7^{\S}$	Controlled rotation (15)
7	Cy3-ADP release ¶	$0.7 - 0.9^{\S}$	Controlled rotation (15)

*All slopes were evaluated at μ M or higher ligand concentration.

† Confidence intervals were calculated from the confidence intervals reported in ref. 14.

‡ Mutant F_1 (β^{E190D}). The reverse reaction (synthesis) is roughly independent of θ (14), hence $\alpha \sim 1$.

§ Qualitative estimation, uncertainty in excess of ~ 0.1 .

¶ Rough estimates both in the presence and absence of P_i in solution. Ligand occupancy was 0 or 1.

Table 3. Comparison of experimentally measured and theoretical predicted Brønsted slopes

Reaction step	Properties*			Experiment	Theory
	λ	ΔG_0^0	W^r	α	α
ATP binding	56	-6.0	-9.1	0.48	0.47
GTP binding	55	-5.4	-9.1	0.56	0.48

*Free energies are given in kcal/mol.

binding and its application to other substeps involving binding and release of a ligand molecule to the ATPase is discussed.

When the elastically compliant rotor is manipulated in these experiments, transitions between reactant and product states of the enzymatic steps occur while the rotor-stator complex undergoes an elastic twisting deformation. In torque-generating enzymatic steps, such as ATP binding, the free energy profiles of steps are perturbed by the elastic energy of twisting, which gives rise to free energy relations as a function of rotor angle.

In the present comparison of theory and experiment, no adjustable parameters were introduced for the results in Tables 3 and 4. Within a harmonic force model for twisting the rotor-stator structure, the theoretical linear dependence of $\ln K$ (or ΔG^0) on the rotor angle is exact. Given the coarse-graining level of present modeling, the quantitative agreement in these tables is reasonable. The kinetic data themselves are approximate, particularly the k data for the steps of GTP binding are sparse, apart from one $k(\theta)$ value (14) and not sufficient to accurately fit an exponential $k(\theta)$ versus θ function. For P_i release at present there are no systematic angle-dependent rate data, the Brønsted slope in Table 3 is based on only two data points, but predictions are made for a future comparison with experiment.

At a molecular level, the binding transition involves a displacement of the ligand through a path inside the β -subunit that leads from the initial weakly bound state to the binding pocket. Presumably as the ligand transitions across the channel, old hydrogen bonds break and new ones form between ligand and host subunit, and within the host subunit itself. A picture in which a hydrogen bond order is conserved along the transition, effectively lowering the TS barrier may apply. Such model for atom transfer (H^+ and CH_3^+) transfer chemical reactions based on the conservation of total bond order has been previously used to describe chemical reactions, and lead to equations similar to those for ATP (16). Atomistic-level treatment permits the detailed exploration of ligand molecule transfer along the path into the pocket (48), and the free energy profile of subunit conformational space coupled to the rotor angle (26, 43), and serve to evaluate and correct the model on which Eqs. 6, 13, and 9 or their bond energy-bond order analogs (16) are based. Atomistic simulations can test the proposed approximate relation of the free energy of activation to the standard free energy of reaction for the individual steps. They can address the coupling between individual processes described phenomenologically in Eqs. 14 and 15. Simulations can calculate the effective torsional elastic constant that appears in the various separations, can calculate the $k_f(\theta)$'s and $K(\theta)$'s for various steps, and can extract the entire $\ln k_f(\theta)$ versus $\ln K(\theta)$ curve and explore its presumed curved nature. In brief, the present formalism may provide a bridge for relating atomistic simulations to the various chemical and mechanical aspects of the ATPases and the details of single molecule behavior.

As noted earlier, the present formulation of the model is not intended to apply to the ATP hydrolysis step, which is believed to involve two or more substeps, rather than just one (28, 30, 50). An α of 0.83 for ATP hydrolysis in tyrosyl-tRNA synthase was inferred by use of mutants, and an explanation of this high α for this reaction, where overall ΔG^0 is small, was given by Warshel, who postulated two transition states of about equal energy with a shallow minimum in between (28). Thereby the first step had a barrier almost equal to the energy to reach the shallow well, and

Table 4. Comparison of free energy changes with respect to angle from stalling experiment with theoretical predictions

Reaction step	Properties*				Experiment [†]		Theory [†]	
	λ	ΔG_0^0	$\theta_f - \theta_i$	$\frac{d \ln K}{d\theta}$	$\frac{d \ln k_f}{d\theta}$	κ	$\frac{d \ln k_f}{d\theta}$	κ
ATP binding	56	-6.0	80°	0.91	0.45	20	0.42	16
GTP binding	55	-5.4	80°	0.84	0.47	20	0.47	15

*Free energies are given in kcal/mol. Properties are estimated from experiment and are independent of columns 4–6.

[†] $d \ln k_f/d\theta$ and $d \ln K/d\theta$ are in units of 1/10° (14). κ is in units of pN · nm (4).

so α was close to unity. Electronic structure calculations in F₁-ATPase of a more ab initio nature (30, 50) indicated at least two TS's, but further studies are needed to explore these TS's, and the valley between them should be treated. Obtaining α via stalling experiments has an advantage over obtaining it via mutations because the latter may also affect λ . A more detailed ab initio theory would also incorporate the structural coupling between the $\alpha_3\beta_3$ ring unit and the rotor, e.g., akin to recent simulations of the electrostatic free energy profile (42, 43).

- Noji H, Yasuda R, Yoshida M, Kinoshita K, Jr (1997) Direct observation of the rotation of F₁-ATPase. *Nature* 386(6622):299–302.
- Yasuda R, Noji H, Yoshida M, Kinoshita K, Jr, Itoh H (2001) Resolution of distinct rotational substeps by submillisecond kinetic analysis of F₁-ATPase. *Nature* 410(6831):898–904.
- Adachi K, et al. (2007) Coupling of rotation and catalysis in F(1)-ATPase revealed by single-molecule imaging and manipulation. *Cell* 130(2):309–321.
- Sielaff H, Rennekamp H, Engelbrecht S, Junge W (2008) Functional halt positions of rotary FOF₁-ATPase correlated with crystal structures. *Biophys J* 95(10):4979–4987.
- Spetzler D, et al. (2009) Single molecule measurements of F₁-ATPase reveal an interdependence between the power stroke and the dwell duration. *Biochemistry* 48(33):7979–7985.
- Watanabe R, Iino R, Noji H (2010) Phosphate release in F₁-ATPase catalytic cycle follows ADP release. *Nat Chem Biol* 6(11):814–820.
- Braig K, Menz R, Montgomery MG, Leslie AG, Walker JE (2000) Structure of bovine mitochondrial F(1)-ATPase inhibited by Mg(2+) ADP and aluminum fluoride. *Structure* 8(6):567–573.
- Boyer PD (1993) The binding change mechanism for ATP synthase—Some probabilities and possibilities. *Biochim Biophys Acta* 1140(3):215–250.
- Senior AE (2007) ATP synthase: Motoring to the finish line. *Cell* 130(2):220–221.
- Weber J (2010) Structural biology: Toward the ATP synthase mechanism. *Nat Chem Biol* 6(11):794–795.
- Walker JE (2013) The ATP synthase: The understood, the uncertain and the unknown. *Biochem Soc Trans* 41(1):1–16.
- Watanabe R, Noji H (2013) Chemomechanical coupling mechanism of F(1)-ATPase: Catalysis and torque generation. *FEBS Lett* 587(8):1030–1035.
- Watanabe R, Noji H (2014) Timing of inorganic phosphate release modulates the catalytic activity of ATP-driven rotary motor protein. *Nat Commun* 5:3486.
- Watanabe R, et al. (2012) Mechanical modulation of catalytic power on F₁-ATPase. *Nat Chem Biol* 8(1):86–92.
- Adachi K, Oiwa K, Yoshida M, Nishizaka T, Kinoshita K, Jr (2012) Controlled rotation of the F₁-ATPase reveals differential and continuous binding changes for ATP synthesis. *Nat Commun* 3:1022.
- Marcus RA (1968) Theoretical relations among rate constants, barriers, and Brønsted slopes of chemical reactions. *J Phys Chem* 72(3):891–899.
- Szabo A (1978) Kinetics of hemoglobin and transition state theory. *Proc Natl Acad Sci USA* 75(5):2108–2111.
- Schweins T, Warshel A (1996) Mechanistic analysis of the observed linear free energy relationships in p21ras and related systems. *Biochemistry* 35(45):14232–14243.
- Marcus RA, Sutin N (1985) Electron transfers in chemistry and biology. *Biochim Biophys Acta* 811(3):265–322.
- Roston D, Islam Z, Kohen A (2014) Kinetic isotope effects as a probe of hydrogen transfers to and from common enzymatic cofactors. *Arch Biochem Biophys* 544:96–104.
- Lewis ES, Hu DD (1984) Methyl transfers. 8. The Marcus equation and transfers between aerosulfonates. *J Am Chem Soc* 106(11):3292–3296.
- Marcus RA (1956) On the electron-transfer reaction. VI. Unified treatment of homogeneous and electrode reactions. *J Chem Phys* 43(2):679–701.
- Marcus RA (1981) Frequency factor in electron transfer reactions and its role in the highly exothermic regime. *Int J Chem Kinet* 13(9):865–872.
- Marcus RA, Siders P (1982) Theory of highly exothermic electron transfer reactions. *J Chem Phys* 82(5):622–630.
- Warshel A, Chu ZT (1990) Quantum corrections for rate constants of diabatic and adiabatic reactions in solutions. *J Chem Phys* 93(6):4003–4015.
- Mukherjee S, Warshel A (2011) Electrostatic origin of the mechanochemical rotary mechanism and the catalytic dwell of F₁-ATPase. *Proc Natl Acad Sci USA* 108(51):20550–20555.
- Weber J, Senior AE (1997) Catalytic mechanism of F₁-ATPase. *Biochim Biophys Acta* 1319(1):19–58.

It is planned to apply the present method and theoretical framework to other single molecule experiments and data, such as the other torque-generating steps probed by stalling, controlled rotation or other advanced techniques, the free energy response in controlled rotation (15) of arbitrary rotation velocity, torque generation (5), and pulling experiments (51). The model can be applied to other ring-shaped NTPases that rotate against a shaftlike structure, such as the helicases or DNA-packaging complexes found in bacteriophage viruses (51).

Methods

The theoretical modeling provided analytic mathematical formulas for the change of rate constants, equilibrium constants, and Brønsted slope with respect to rotor angle. The theoretical values of these quantities were calculated using properties such as angular displacements, elastic constants, and the energetics of free rotation from ensemble and single molecule experiments. These quantities were compared with their experimental counterparts from previously published stalling experiments.

ACKNOWLEDGMENTS. We thank Drs. Long Cai, Attila Szabo, David Thirumalai, and Arieh Warshel for their helpful comments. The authors would like to acknowledge support from the Office of the Naval Research, the Army Research Office, and the James W. Glanville Foundation.

- Warshel A, Schweins T, Fothergill M (1994) Linear free energy relationships in enzymes. Theoretical analysis of the reaction of tyrosyl-tRNA synthetase. *J Am Chem Soc* 116(19):8437–8442.
- Dittrich M, Hayashi S, Schulten K (2004) ATP hydrolysis in the β_{TP} and β_{DP} catalytic sites of F₁-ATPase. *Biophys J* 87(5):2954–2967.
- Hayashi S, et al. (2012) Molecular mechanism of ATP hydrolysis in F₁-ATPase revealed by molecular simulations and single-molecule observations. *J Am Chem Soc* 134(20):8447–8454.
- Pänke O, Cherepanov DA, Gumbiowski K, Engelbrecht S, Junge W (2001) Viscoelastic dynamics of actin filaments coupled to rotary F-ATPase: Angular torque profile of the enzyme. *Biophys J* 81(3):1220–1233.
- Wächter A, et al. (2011) Two rotary motors in F-ATP synthase are elastically coupled by a flexible rotor and a stiff stator stalk. *Proc Natl Acad Sci USA* 108(10):3924–3929.
- Wolfe S, et al. (1981) Theoretical studies of S_N2 transition-states. 2. Intrinsic barriers, rate-equilibrium relationships, and the Marcus equation. *J Am Chem Soc* 103(25):7694–7696.
- Murdoch JR, Magnoli DE (1982) Kinetic and thermodynamic control in group transfer reactions. *J Am Chem Soc* 104(14):588–600.
- Murdoch JR (1983) A simple relationship between empirical theories for predicting barrier heights of electron-transfer, proton-transfer, atom-transfer, and group-transfer reactions. *J Am Chem Soc* 105(8):2159–2164.
- Murdoch JR (1983) Barrier heights and the position of stationary-points along the reaction coordinate. *J Am Chem Soc* 105(9):2667–2672.
- Donella J, Murdoch JR (1984) Application of Marcus-like equations to group-transfer reactions – A theoretical test of intrinsic barrier additivity and the square relationship. *J Am Chem Soc* 106(17):4724–4735.
- Chidsey CED (1991) Free energy and temperature dependence of electron transfer at the metal-electrolyte interface. *Science* 251(4996):919–922.
- Kuharski RA, et al. (1988) Molecular model for aqueous ferrous-ferric electron transfer. *J Chem Phys* 89(5):3248–3257.
- Menzeleev AR, Ananth N, Miller TF, 3rd (2011) Direct simulation of electron transfer using ring polymer molecular dynamics: Comparison with semiclassical instanton theory and exact quantum methods. *J Chem Phys* 135(7):074106.
- Oster G, Wang H (2000) Reverse engineering a protein: The mechanochemistry of ATP synthase. *Biochim Biophys Acta* 1458(2-3):482–510.
- Mukherjee S, Warshel A (2015) Dissecting the role of the γ -subunit in the rotary-chemical coupling and torque generation of F₁-ATPase. *Proc Natl Acad Sci USA* 112(9):2746–2751.
- Mukherjee S, Bora RP, Warshel A (2015) Torque, chemistry and efficiency in molecular motors: A study of the rotary-chemical coupling in F₁-ATPase. *Q Rev Biophys*, 10.1017/S0033583515000050.
- Adamson A (1973) *A Textbook of Physical Chemistry* (Academic Press, New York).
- Barker JA, Henderson D (1976) What is a “liquid”? understanding the states of matter. *Rev Mod Phys* 48(4):587–671.
- Nishizaka T, et al. (2004) Chemomechanical coupling in F₁-ATPase revealed by simultaneous observation of nucleotide kinetics and rotation. *Nat Struct Mol Biol* 11(2):142–148.
- Masaie T, Koyama-Horibe F, Oiwa K, Yoshida M, Nishizaka T (2008) Cooperative three-step motions in catalytic subunits of F(1)-ATPase correlate with 80 degrees and 40 degrees substep rotations. *Nat Struct Mol Biol* 15(12):1326–1333.
- Okazaki K-i, Hummer G (2013) Phosphate release coupled to rotary motion of F₁-ATPase. *Proc Natl Acad Sci USA* 110(41):16468–16473.
- Junge W, Sielaff H, Engelbrecht S (2009) Torque generation and elastic power transmission in the rotary F₀F₁-ATPase. *Nature* 459(7245):364–370.
- Dittrich M, Hayashi S, Schulten K (2003) On the mechanism of ATP hydrolysis in F₁-ATPase. *Biophys J* 85(4):2253–2266.
- Yu J, Moffitt J, Hetherington CL, Bustamante C, Oster G (2010) Mechanochemistry of a viral DNA packaging motor. *J Mol Biol* 400(2):186–203.